Received 6 June 2008
Revised 6 January 2009,
28 May 2009
Accepted 21 July 2009

Modelling and simulation of flow boiling heat transfer

Fabian Krause, Sven Schüttenberg and Udo Fritsching
Faculty of Production Engineering, Chemical Engineering Department, University of Bremen, Bremen, Germany

Abstract

Purpose – The purpose of this paper is to describe the development and application of a numerical model for analysis of flow boiling phenomena and heat transfer.
Design/methodology/approach – For flow boiling processes, the fluid and vapour flow regimes in connection with the conjugate heat and mass transfer problem for specimen quenching through the entire boiling curve is modelled. Vaporisation and recondensation, the vapour fraction distribution and vapour movement with respect to the liquid are considered in the calculation of the two-phase flow and heat transfer process. The derived flow boiling model is based on a mixture model and bubble crowding model approach for two-phase flow. In addition to the conventional mixture model formulation, here special model implementations have been incorporated that describe: the vapour formation at the superheated solid-liquid interface, the recondensation process of vapour at the subcooled vapour-liquid interface, the mass transfer rate in the different boiling phases and the microconvection effect in the nucleate boiling phase resulting from bubble growth and detachment.
Findings – The model prediction results are compared with experimental data for quenching of a circular cylinder, showing good agreement in boiling state and heat transfer coefficient distribution. Simulation and experiments lead to a better understanding of the interaction of incident flow in the boiling state and the resulting heat transfer.
Research limitations/implications – Fluid temperatures in the range of 300-353 K and specimen wall temperatures up to 1,000 K are considered.
Practical implications – Flow boiling is an efficient heat transfer process occurring in several technical applications. Application background of the model development is in quenching of complex metallic specimen geometries in liquids subject to fast changing heat fluxes.
Originality/value – A general model for the complex two-phase boiling heat transfer at high wall temperatures and fast flow conditions that can be used in engineering applications does not yet exist. The results provide detailed information describing the non-uniform phase change during the complete quenching process from film boiling to pure convection.
Keywords Flow, Boiling, Heat transfer, Simulation, Modelling
Paper type Research paper

Nomenclature

E	enthalpy ($J\,kg^{-1}\,K^{-1}$)	p	pressure ($N\,m^{-2}$)
F	force field (N)	r	radius (m)
g	gravity ($m\,s^{-2}$)	S	source/sink
Δhv	specific heat ($J\,kg^{-1}$)	T	temperature (K)
h	height (m)	v	velocity ($m\,s^{-1}$)
q	heat flux ($W\ m^{-2}$)	$\vec{v}$	velocity vector

The quenching modelling project has been funded by the Arbeitsgemeinschaft industrieller Forschungsvereinigungen AiF within the project "Intensive Quenching" and in the Sonderforschungsbereich "Distortion Engineering" of the Deutsche Forschungsgemeinschaft DFG at the University of Bremen and the Institute for Materials Science, Bremen. The support is gratefully acknowledged.

International Journal of Numerical Methods for Heat & Fluid Flow
Vol. 20 No. 3, 2010
pp. 312-331

0961-5539
DOI 10.1108/09615531011024066

$\vec{n}$ normal vector

Greek letters

α heat transfer coefficient ($W\,m^{-2}\,K^{-1}$)

β mass transfer coefficient ($m\,s^{-1}$)

μ viscosity (Pa s)

ρ density ($kg\,m^{-3}$)

Subscripts

ax axial incident flow

dr drag force

liq liquid

m mixture

n phase index, 1 = liquid, 2 = vapour

max maximum

rad radial incident flow

rel relative

turb turbulent

sat saturation

vap vapour

w wall

1. Introduction

Quenching is the fast cooling process of heated (up to 1,200 K) metal specimen and components to achieve specific microstructures of the material. In order to achieve high cooling rates most quenching processes are performed in liquid media. Quenching fluids such as water, quenching oils or polymers are typically used in this context. For a proper technical description and analysis of the process, the most limiting factors of the heat transfer analysis are the complex boiling and rewetting phenomena that occur on the solid surface during the quenching process in liquids. These processes up to date are not possible to prescribe as they depend on a lot of influencing parameters as specimen geometry and surface condition (roughness), liquid temperature and liquid condition (purity) and others.

Figure 1 illustrates the quenching process of a steel cylinder in a stagnant water reservoir. An immersed cylinder is seen in different stages of the cooling process. The initial temperature of the specimen is 1,153 K. From left to right the pictures illustrate the local boiling state at the surface of the cylinder at different times. During the quenching process in the liquid different boiling states occur. Immediately after the dipping of the cylinder into the liquid, the surface temperature is above the Leidenfrost temperature and a continuous vapour film covers the surface (Figure 1a). After a few seconds the rewetting of the surface starts, typically in this arrangement from the bottom edge (Figure 1b) moving upwards, later also from the top edge (Figure 1c) of the cylinder moving downwards. At the rewetting front nucleate boiling occurs. In the rewetted area, the heat transfer process is pure single phase convective. The specimen is cooled until equilibrium with the water temperature is achieved.

The boiling heat transfer in a quenching process depends on phase transition, fluid dynamics and heat transport. For an optimum design of the quenching process, the temporal and spatial flow field and heat transfer must be predicted. This requires knowledge of the local hydrodynamic conditions and mass transfer phenomena. High resolution computational fluid dynamics (CFD) is used here because only an integral calculation gives an estimation of this highly complex and unsteady process. The analysis is based on a two-phase flow approach (liquid and vapour) with heat and mass transfer and phase change.

With respect to the great importance of boiling heat transfer analysis in many industrial processes, several models and correlations for boiling heat transfer

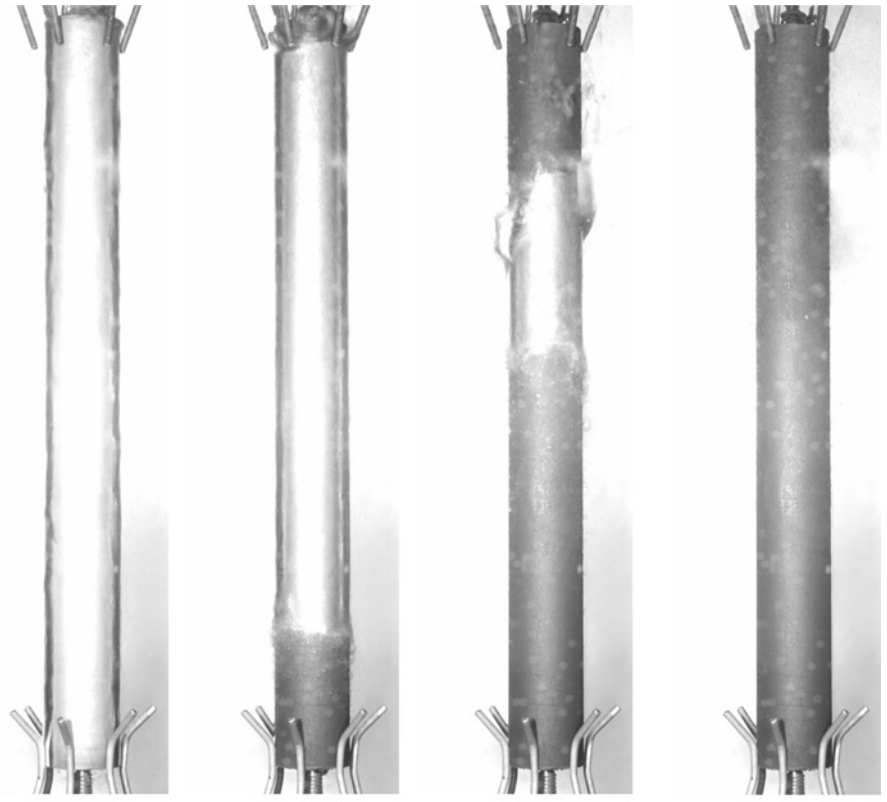

Notes: Material 20MnCr5, fluid: water; fluid temperature = 70 °C; cylinder initial temperature = 880 °C, cylinder dimensions l = 200 mm and d = 20 mm

Figure 1.
Quenching of a circular cylinder in a stagnate water reservoir

description already have been developed. These models generally can be classified into two groups, empirical and theoretical (mechanistic) models, respectively.

1.1 Empirical models

Empirical boiling models typically based on experimental data exist, e.g. for the different stages of pool boiling (Rohsenow, 1952; Cooper, 1984), boiling inside and outside of tubes (Weisman and Pei, 1983; Celata *et al.*, 1997), and for different types of heat exchangers (e.g. VDI, 2002). Empirical modelling offers useful results for steady-state cases and only in the limited temperature range and geometries that they have been developed for. Extrapolating these correlations to other geometries, differing fluids or other temperature ranges is typically not possible. Most empirical models are rather complex and give very detailed views of the boiling process; however, these models are often based on questionable assumptions. Empirical models are typically only valid for the variation of a single parameter and not for the interaction of different parameters. Most models are valid only for the nucleated boiling regime up to the critical heat flux (CHF). Some models exist for film or flow boiling regimes in tubes or

at the outside of tubes (Auracher and Marquardt, 2002; Elias and Yadigaroglu, 1977; Yadigaroglu, 2005).

Typically, empirical models describe heat flux controlled cases because of their relevance in heat exchangers and nuclear power stations. In quenching processes, the transient boiling phases depend on the wall temperature and the flow conditions.

1.2 Theoretical models

Theoretical models typically analyse in detail the local mechanisms in boiling processes and describe the behaviour of the liquid and vapour based on thermodynamic and physical laws. Consequently, every boundary condition has to be known and every interaction has to be described or modelled. Accordingly, high spatial and temporal resolutions are needed, leading to high computational costs.

Within the nucleate boiling process, due to the development of computer technology and solver algorithms on one hand and measurement techniques on the other hand, it is possible to predict the behaviour of single bubbles and the vapour film interface in detail. Dhir (2001) and Dhir and Gihun (2007) developed different models and validated these in experiments for initial nucleation boiling as well as for film boiling. The boiling model based on the Arbitrary Lagrangian-Eulerian method as developed by Stephan and Fuchs (2007) is able to predict the initial nucleate boiling and the generation, departure and rising of single bubbles for several different liquids. The method needs a high spatial and temporal resolution, expensive computing time and *a priori* known empirical data like the nucleation site density. Esmaeeli and Tryggvason (2004) describe a model based on direct numerical simulation (DNS) for stable film boiling. Because this model requires high resolution, it is limited to a spatial surface region of a few square millimetres.

The mechanistic models help understanding of the physics of boiling, but are (so far) not useable for applied simulations in engineering applications.

A general model for the complex two-phase boiling heat transfer at high wall temperatures and fast flow conditions that can be used in engineering applications does not yet exist. The reason is the variety of occurring boiling phenomena along with the different phase interactions at the heated wall. Simulation and experiments lead to a better understanding of the interaction of incident flow in the boiling state and the resulting heat transfer.

In conclusion the problem is that empirical models give only a very rough value for a small part of the boiling curve, while numerical models which resolve the phase boundary use way to much computational afford to be feasible for engineering problems in quenching applications.

The CFD simulation of quenching processes is well established for single phase heat transfer in gas quenching (e.g. Schmidt and Fritsching, 2007). Here a first CFD model for quenching in evaporating liquids is presented. It allows calculating a local heat transfer coefficient from the local temperature and flow conditions considering the isolating effect of vapour. This model is valid for all temperatures and boiling phases that may occur in a typical industrial quenching process.

2. Description of the model

The developed model for analysis of transient boiling determines the temporal and spatial heat flux and phase fraction during the quenching process in a two-phase fluid (liquid and vapour) using a mixture model approach.

2.1 Bubble crowding model

The employed mixture model is a simplified multiphase model. It can model n phases (fluid or particulate) by solving the momentum, continuity and energy equations for the mixture, the volume fraction equations for the secondary phases and algebraic expressions for the relative velocities.

This model, like the VOF model, uses a single-fluid approach. It differs from the VOF model in two respects:

(1) The phases are allowed to be interpenetrating. The volume fractions for a control volume can therefore be equal to any value between 0 and 1, depending on the space occupied by primary and secondary phase.

(2) The phases are allowed to move at different velocities, using the concept of slip velocities.

The mixture model is a good substitute for the full Eulerian multiphase model in several cases. A simpler model like the mixture model can perform as well as a full multiphase model while solving a smaller number of variables than the full multiphase model (Fluent, 2006).

The mixture model solves the continuity equation for the mixture, the momentum equation for the mixture, the energy equation for the mixture and the volume fraction equation for the secondary phases, as well as algebraic expressions for the relative velocities.

Continuity:

$$\frac{\partial}{\partial t}(\rho_m) + \nabla \cdot (\rho_m \vec{v}_m) = S_m \tag{1}$$

Momentum:

$$\frac{\partial}{\partial t}(\rho_m \vec{v}_m) + \nabla \cdot (\rho_m \vec{v}_m \vec{v}_m) = -\nabla p \nabla [\mu_m (\vec{v}_m + \vec{v}_m^T)] + \rho_m \vec{g} + \vec{F} + \nabla \cdot \sum_{k=1}^{n} (\alpha_k \rho_k \vec{v}_{dr,k} \vec{v}_{dr,k}) \tag{2}$$

Energy:

$$\frac{\partial}{\partial t} \sum_{k=1}^{n} (\alpha_k \rho_k E_k) + \nabla \cdot \sum_{k=1}^{n} (\alpha_k \vec{v}_k (\rho_k E_k + p)) = \nabla \cdot (k_{eff} \nabla T) + S_E \tag{3}$$

The energy equation summarises over all phases resulting in a single temperature for all phases in one computational cell.

Continuity and momentum equation use averaged values for density, velocity and viscosity. The values are averaged by phase fraction α and weighted by density ρ as:

$$\phi_m = \phi_{vap} \alpha_{vap} \rho_{vap} + \phi_{liq} \alpha_{liq} \rho_{liq} \tag{4}$$

The volume fraction α, is defined as:

$$\alpha_{vap} = \frac{V_{vap}}{V_{vap} + V_{liq}}$$
$$\alpha_{liq} = \frac{V_{liq}}{V_{vap} + V_{liq}} \quad (5)$$

The mixture model does not resolve the location of the phase boundary, but instead calculates a local volume fraction distribution. The secondary (vapour) phase is assumed to be a dispersed phase with constant diameter (spherical bubbles). For high wall heating, no real vapour film immerses the wall, but an intense crowding of bubbles occurs (as illustrated in Figure 2). This model results in almost the same effect on the heat transfer mechanisms during film boiling as a continuous vapour film model. The mixture model resembles the bubble crowding model for CHF (Weisman and Pei, 1983). In the nucleate boiling regime, the dispersed behaviour of the two-phase flow is directly reflected. In the convective heat transfer regime only the single phase liquid analysis is needed.

For description of flow-boiling phenomena, the combined mixture model and bubble crowding approach has been extended here to properly describe:

- the vapour formation at the superheated solid-liquid interface;
- the recondensation process of vapour at the subcooled vapour-liquid interface;
- the mass transfer rate in the different boiling phases; and
- the microconvection effect in the nucleate boiling phase resulting from bubble growth and detachment.

These model implementations will be described in the following.

2.2 Phase change model

Some important effects and terms in the energy and continuity equations are necessary to take into account the phase change behaviour. The implementation of the derived

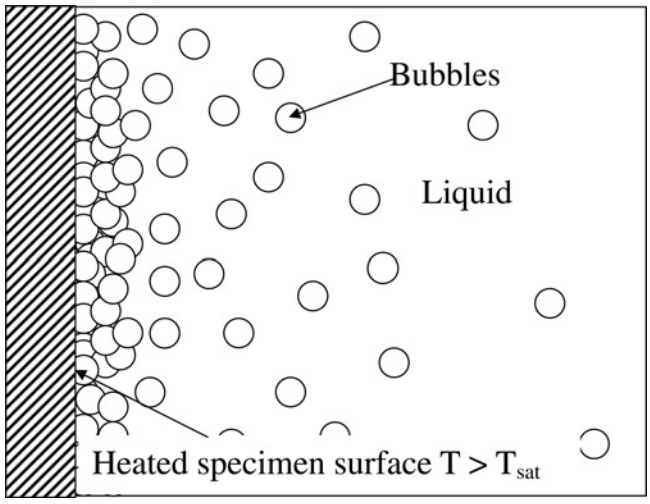

Figure 2.
Bubble crowding model

sink and source terms is shown in Figure 3. At temperatures above the saturation temperature, phase change from liquid to vapour occurs (evaporation) and *vice versa* at temperatures below the saturation temperature (condensation). A pressure dependency of evaporation (e.g. due to cavitation) is not taken into account in this model. There is no need for *a priori* treatment of nucleation sites or a liquid-vapour interface to onset boiling. This assumption is feasible in quenching applications because the surfaces are technically rough and the liquids are not pure, resulting in a great number of nucleation and condensation sites.

The phase change mass transfer is solved by sink and source terms in the continuity equation (1) as:

$$\begin{array}{ll} T \geq T_{sat} \rightarrow \text{Evaporation} & T < T_{sat} \rightarrow \text{Condensation} \\ S_{mass,vap} = +\beta\alpha_{liq}\rho_{liq}\dfrac{T - T_{sat}}{T_{sat}} & S_{mass,vap} = -\beta\alpha_{vap}\rho_{vap}\dfrac{T_{sat} - T}{T_{sat}} \\ S_{mass,liq} = -S_{mass,vap} & S_{mass,liq} = -S_{mass,vap} \end{array} \quad (6)$$

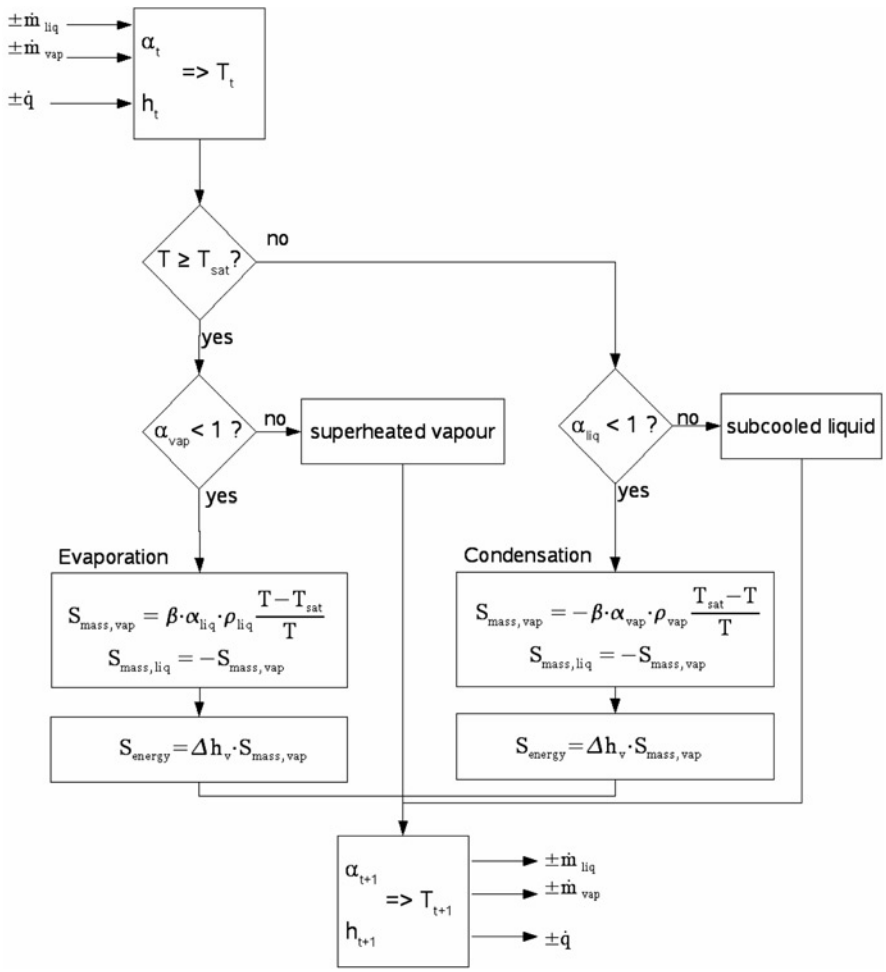

Figure 3.
Sink and source terms

The intensity of evaporation is a function of superheat, gas-liquid interface and the mass transfer coefficient. Because there is no distinct gas-liquid interface in the mixture model, the mass fraction (α_n. ρ_n) is used as exchange parameter. The superheat is taken into account by the term $[(T - T_{sat})/T]$. The mass transfer coefficient β in $(m^3\,(m^2\,s)^{-1})$ is to be defined as function of the local temperature (equation (8)).

Though there is a change in the phase fraction α, the total mass source is zero, because the vapour and liquid mass sources are balanced. Evaporation and condensation cause a jump in enthalpy due to the latent heat Δh_v. The latent heat is taken into account by a sink and source term in the energy equation (3) as:

$$S_{Energy} = \Delta h_v \cdot S_{mass,vap} \tag{7}$$

The mass transfer coefficient β in equation (6) reflects the local evaporation and condensation rate and combines the influence of unknown factors e.g. bubble size and nucleation size density. A first run with fixed $\beta = 1\,m^3\,m^{-2}\,s^{-1}$) give good representation of the boiling phases expected (from experiments and literature) but underestimated the heat transfer coefficient in the critical heat transfer region. To improve the representation of the CHF region a temperature-dependent function $\beta(T)$ is implemented. A first estimated for the coefficients β_0, β_{crit} and β_{film} as well as the temperatures T_{crit} and T_{leid} are found by the calculation with $\beta = 1$. The improved values (Table I) are defined by iterative sensitivity analyse comparing the results with experiments and literature.

The chosen factors are validated for the examined case of a cylinder with radial or axial flow. Due to the calculation on finite volumes we assume that this will also be valid for more complex geometries with similar local conditions (temperature and flow fields). For liquids different to water (polymers, oil) different values for β_0, β_{crit} and β_{film} as well as T_{crit} and T_{leid} expected but can found in the same way, tacking $\beta = 1$ as a first estimation:

$$\beta(T) = \begin{cases} \beta_0 & (T < T_{sat}) \quad \text{condensation} \\ \beta_0 + (\beta_{crit} - \beta_0)\left(\dfrac{T - T_{sat}}{T_{crit} - T_{sat}}\right) & (T_{sat} \le T < T_{crit}) \quad \text{nucleate boiling} \\ \beta_{crit} & (T = T_{crit}) \quad \text{critical heat flux} \\ \beta_{crit} + (\beta_{film} - \beta_{crit})\left(\dfrac{T - T_{crit}}{T_{leid} - T_{crit}}\right) & (T_{crit} < T < T_{leid}) \quad \text{transient boiling} \\ \beta_{film} & (T \ge T_{leid}) \quad \text{film boiling} \end{cases} \tag{8}$$

The bubble displacement from the wall relative to the liquid during nucleate boiling results in a microconvection effect that enhances the local heat transfer process. This

β_0	$1\,m\,s^{-1}$
β_{crit}	$10\,m\,s^{-1}$
β_{film}	$1\,m\,s^{-1}$
T_{crit}	400 K
T_{leid}	650 K

Table I. Mass transfer coefficients and temperatures for $\beta(T)$ (equation (8)) defined by a sensitivity analysis

effect is taken into account by implementing a function for the relative vapour velocity normal to the wall during the bubble displacement process in the nucleate boiling regime in order to reflect microconvection effects. The velocity tangential to the wall is set to zero, while the velocity normal to the wall is a function of generated vapour mass divided by the maximum vapour generation. For the maximum generated vapour the relative velocity is $1\,\mathrm{m\,s^{-1}}$. This values have been defined by a sensitivity analysis (Table II):

$$\begin{aligned} \vec{v}_{rel,vap} &= \begin{pmatrix} v_{tangential} \\ v_{normal} \end{pmatrix} \\ v_{rel,vap,tangential} &= 0 \\ v_{rel,vap,normal} &= v_o \left(\frac{S_{mass,vap}}{S_0} \right) \end{aligned} \tag{9}$$

2.3 Implementation in CFD

The model implementation is used to drive quenching process simulations for a cylinder with a diameter of 20 mm and a height of 100 mm (Figure 4) that is immersed either in a stagnant water bath or is subjected to a superficial axial liquid velocity during quenching. The simulation is performed in two dimensions in an axis symmetric formulation. By grid independency tests it has been confirmed that for a correct prediction of the vapour film at the wall, the size of the first cell has to be smaller than 0.1 mm in wall normal direction. In axial direction the size can be ten times larger (Figure 5). The grid tests also show that the sharp step in the grid size should not be in the region of the vapour film to avoid numerical inaccuracies. To further reduce the influence of the grid adaptation a sizing function may be helpful. To reduce the influence of in- and out-flow boundaries, a height of the liquid pool of 0.2 m with a radius of 0.05 m is necessary, resulting in a grid of approximately 20,000 cells. The Reynolds number in this cases is in the range of $10^4 < Re < 2{\cdot}10^5$ where still laminar flow is assumed.

The model is implemented for computations within the mixture model in the CFD-code Fluent 6.3. The additional sink and source terms are implemented via user-defined functions.

The conservation equations are solved using a pressure-based implicit PISO pressure-velocity coupling, where the convective terms are discretised using second-order upwind with volume fraction Quick. A time step of 1 ms is used for the unsteady simulations.

3. Results and discussion

The developed model describes the mass, energy and momentum transport during boiling with additional terms in the continuity energy and momentum equations. This allows to predict the local heat flux for the entire boiling curve (film, transient and nucleate boiling, and pure convection) within one model.

Two different cases are examined, steady-state (constant wall temperature) and transient (continuous cooling of a specimen) heat transfer. The results of the simulations are compared with data from experiments and literature.

Table II.
Coefficients for equation (9)

v_0	$1\,\mathrm{m\,s^{-1}}$
S_0	$S_{mass,vap,max}$

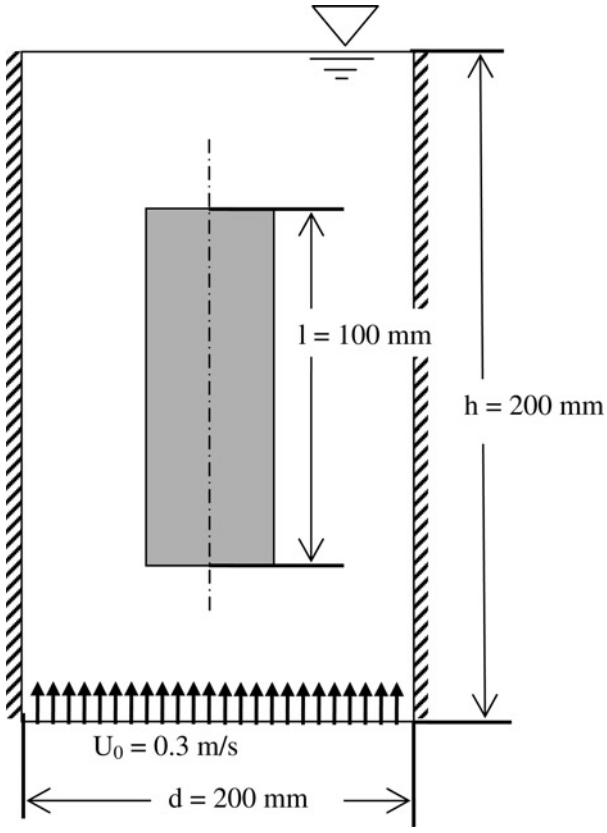

Figure 4.
Computational domain

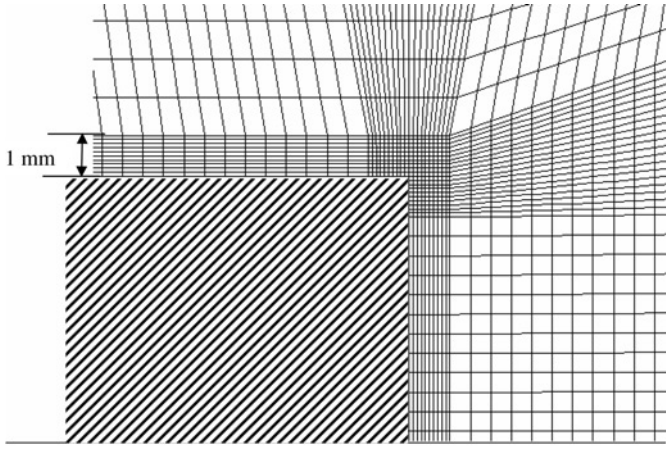

Note: Detail at the upper right corner of the cylinder

Figure 5.
Computational grid
arrangement

3.1 Steady-state simulations

In steady-state simulations, the temperature of the cylinder is prescribed and constant. Also for these steady-state boundary conditions an unsteady simulation is necessary, because of the transient nature of the boiling process. For a single point on the cylinder surface strong fluctuations of the heat flux will be achieved, as shown in Figure 6 for a point at the half height of the cylinder. Typically, temporally averaged values are used for the examination of the local heat flux.

Figure 7 shows results for the averaged calculated radial vapour fraction distribution at the half height of the cylinder at different wall (cylinder) temperatures. The simulations have been performed in an axial flow of $0.3\,\mathrm{m\,s^{-1}}$ at three different cylinder temperatures ($T_{cylinder}$ 400, 500 and 1,000 K). The temperature of the entering liquid is fixed to $T_{liquid} = 293\,\mathrm{K}$. For comparison photos of the different boiling phases on a cylinder are given in the figure that show a qualitative agreement with the simulation results.

The diagram highlights the differences in the radial phase fraction distributions for temperatures above and below the Leidenfrost point. At a wall temperature 1,000 K a dense vapour film at the surface (vapour fraction ≈ 1 at $r = 0$) and few vapour outside the vapour film indicates film boiling (wall temperature above the Leidenfrost point) while at $T_{wall} = 500$ and 400 K the wall vapour fraction below 1 indicates transient, respectively, nucleate boiling.

The effect of the different phase fraction distributions to the heat transfer represents the following diagram. Figure 8 shows results for the calculated average (spatial and temporal) heat flux at the cylinder wall at different wall (cylinder) temperatures and for different liquid temperatures. The simulations have been performed for a cylinder in an axial flow of $0.3\,\mathrm{m\,s^{-1}}$ as a result of a series of steady-state simulations, each preformed at a single cylinder temperature. The cylinder temperature and the temperature of the entering liquid are varied in the range of $300\,\mathrm{K} < T_{cylinder} < 800\,\mathrm{K}$ and $293\,\mathrm{K} < T_{liquid} < 353\,\mathrm{K}$, respectively.

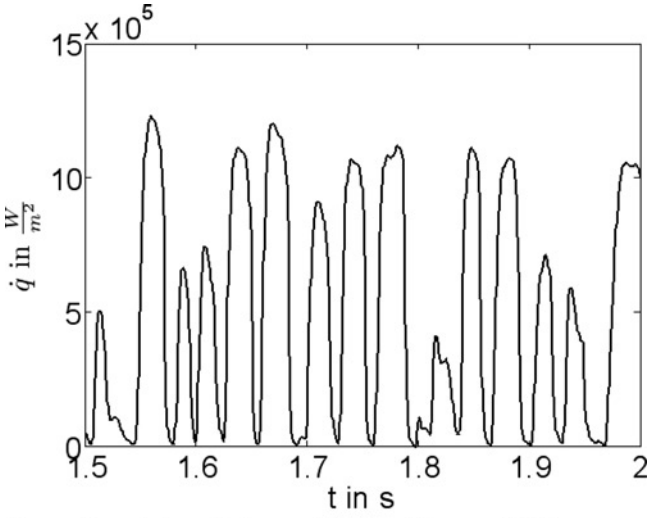

Notes: $V_{ax} = 0.3\,\mathrm{ms^{-1}}$, $T_{liquid} = 332\,\mathrm{K}$ and $T_{solid} = 500\,\mathrm{K}$

Figure 6.
Local heat flux at a single point at the half height of the cylinder

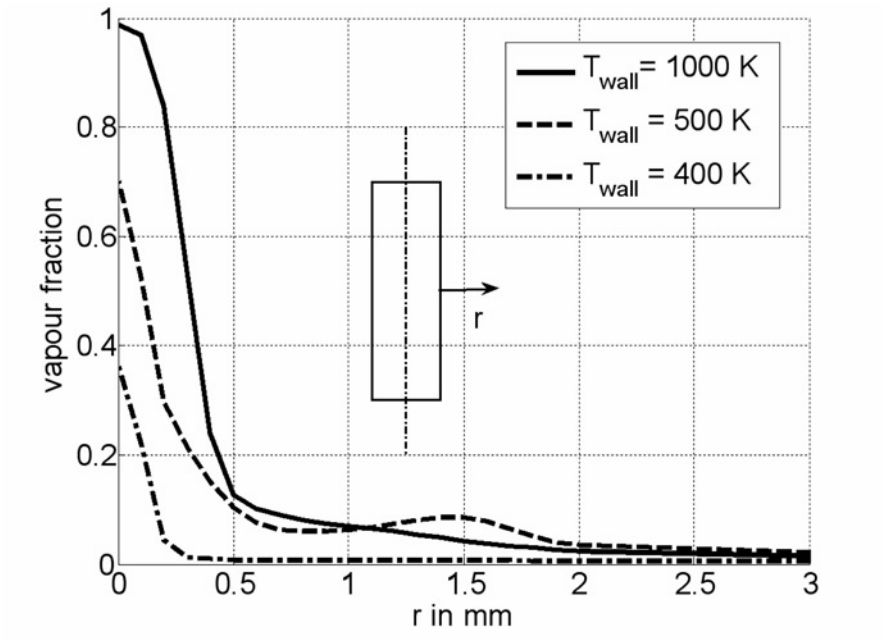

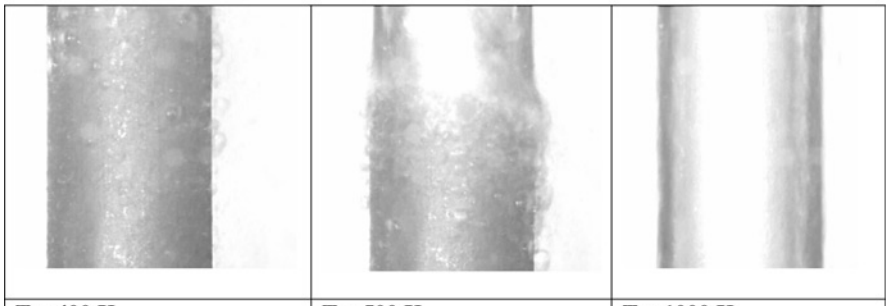

T = 400 K	T = 500 K	T = 1000 K
nucleate boiling	transient boiling	film boiling

Notes: $V_{ax} = 0.3\,ms^{-1}$ and $T_{fl} = 293\,K$

Figure 7.
Radial vapour fraction at the half height of a vertical cylinder and photos of the different boiling phases

From these results it is to be concluded that the main phenomena of the different boiling and heat transfer regimes are reflected. A local minimum in the heat transfer rate at $\Delta T \approx 200\text{-}250\,K$ indicates the Leidenfrost point while the CHF is achieved at $\Delta T \approx 50\text{-}120\,K$. The shift of the Leidenfrost point with increasing liquid temperature (higher subcooling) and the increasing of the CHF with increasing subcooling follows the same trend as described by Celata *et al.* (2007).

Comparing the calculations with the experimental results from Auracher and Marquardt (2004) show a good representation of the boiling curve by the present model. In the experiments the cooling process from superheating through the different

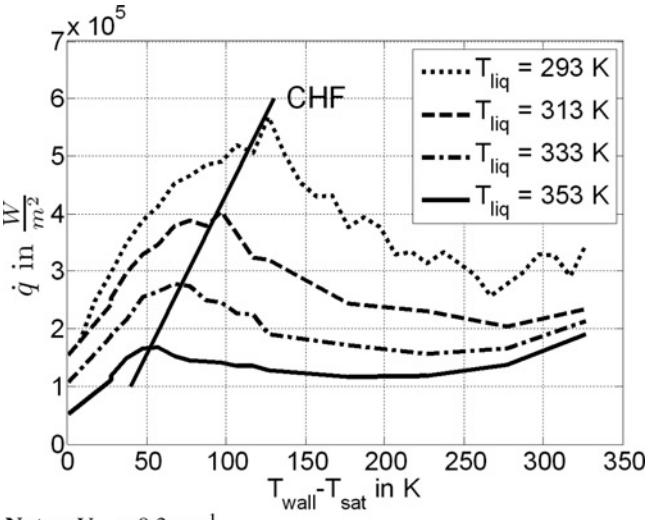

Notes: $V_{ax} = 0.3\,ms^{-1}$

Figure 8.
Averaged heat flux of a vertical cylinder

boiling regimes has been observed. The simulation result of the heat transfer coefficient value agree for film and initial nucleate boiling but differ in the CHF ($0.6 \times 10^6\,W\,m^{-2}$ instead of $1.4 \times 10^6\,W\,m^{-2}$). Reasons for this difference may be due to the averaging procedure and the simplification by using steady-state simulations. The measurements of Auracher and Marquardt (2002) show a strong increase of the CHF for transient heat transfer. The CHF is higher by a factor of four than the one in the steady-state case as calculated here.

When plotting the maximum of the non-averaged heat transfer for a single point as shown in Figure 9, the value of $1.1 \times 10^6\,W\,m^{-2}$ like that measured by Celata *et al.*

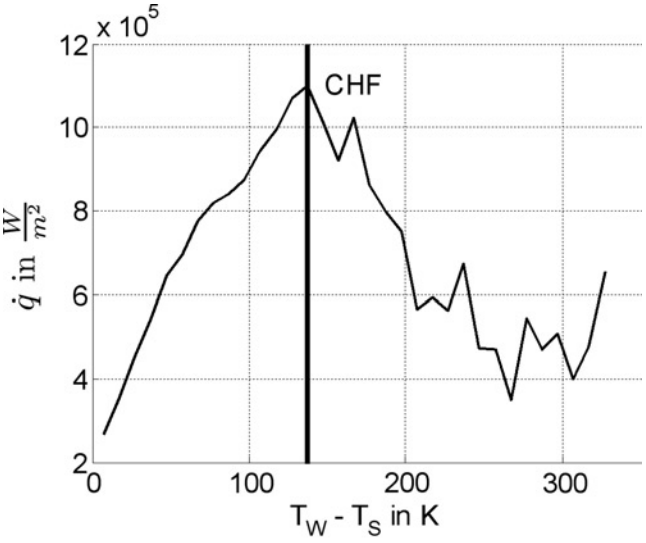

Notes: $V_{ax} = 0.3\,ms^{-1}$ and $T_{fl} = 293\,K$

Figure 9.
Maximum heat flux of a single point at a vertical cylinder at the half height

(2007) and close to the value of $1.4 \times 10^6\,\mathrm{W\,m^{-2}}$ measured by Auracher and Marquardt (2004) is achieved.

3.2 Influence of model parameters

Different calculations are performed to show the influence of the chosen model parameters.

3.2.1 Radiation. The influence of radiation heat transfer at the CHF is negligible. Figure 10 shows that, at the CHF, the calculated ratio of radiation heat flux to the total heat flux is less than 2 per cent. Also at 800 K the radiation is less than 10 per cent. Only for massive superheated components with an intensive film boiling phase radiation should not be omitted.

3.2.2 Mass transfer coefficient β. An increasing mass transfer coefficient β (equation (8)) results in an increase in the maximum wall heat transfer coefficient for β up to 10 but will decrease for β > 10 (see Figure 11). The reason for this behaviour is

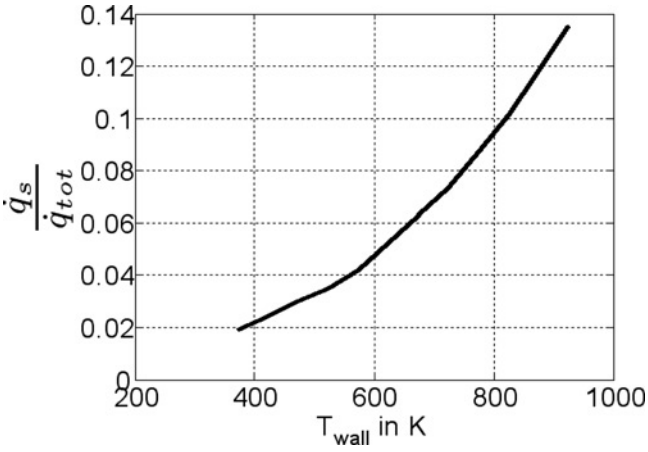

Figure 10.
Ratio of radiation heat flux to total heat flux

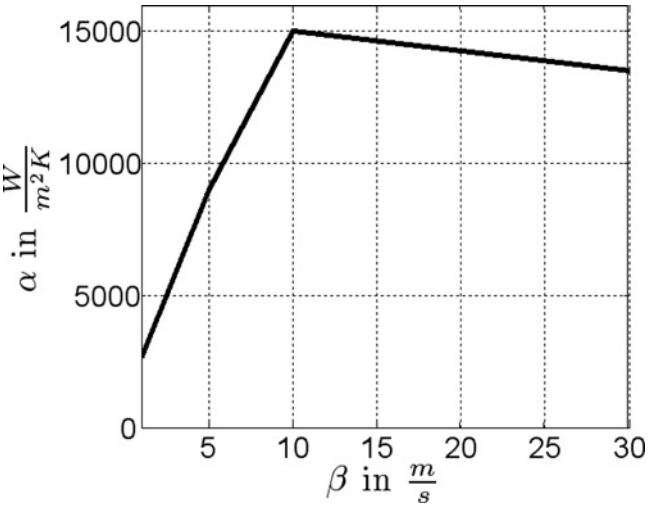

Figure 11.
Influence of mass transfer coefficient β on the maximum surface heat transfer coefficient

such that a higher β increases the vapour production. For $\beta > 10$ this will lead to a vapour film, reducing the heat transfer.

3.2.3 Vapour slip velocity. With the additional vapour slip velocity (equation (9)) the effect of microconvection is taken into account. Figure 12 shows the effect of the vapour slip velocity on the heat transfer coefficient. Without vapour slip velocity the boiling film is too permanent and needs too long to disappear. This will underestimate the heat transfer. If the assumption for the relative vapour velocity is too high, no boiling film will occur and the heat transfer for high wall superheating will overestimate.

3.3 Transient simulations

To analyse the quenching process during the cooling of specimen, transient simulations are necessary instead of steady-state simulations. In the simulations for transient cooling, a cylinder with a homogenous start temperature is quenched in a liquid with a fixed liquid temperature at the inlet. In this case the resulting heat flux inside the cylinder is taken into account and the conjugate heat transfer problem is solved. Figure 13 shows the temperature field in the cylinder and flow field vectors in the fluid at $t = 7.5$ s.

Typical local temperature distributions for the surface and the centre of the cylinder (at the half height) are plotted in Figure 14. In the period from 10 to 20 s, a very slow decrease in temperature occurs, indicating the film boiling regime in this time with lower heat transfer rates. According to this, the heat flux in this period shows a local minimum (Figure 15). For $t > 20$ s the heat flux increases as a result of rewetting and the transient and nucleate boiling phases. The local collapse of the vapour film can be seen in the sequence in Figure 16.

The results show that the model is able to predict the whole quenching process of a component by coupling the heat transfer in the solid and in the fluid considering the different boiling phenomena.

Comparison of the simulation results with quenching processes experiments from Stich and Tensi (1995) for quenching of a cylinder is illustrated in Figure 17. The distinct heat transfer phases as film boiling, nucleate boiling and pure convection

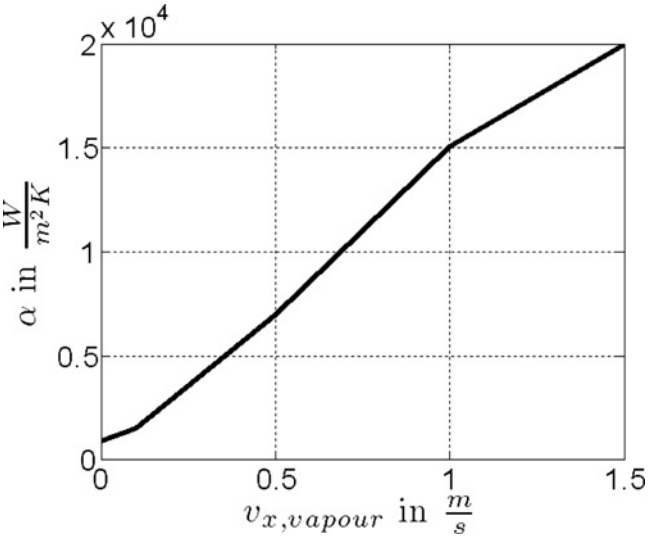

Figure 12.
Influence of relative normal vapour velocity at the wall on the maximum surface heat transfer coefficient

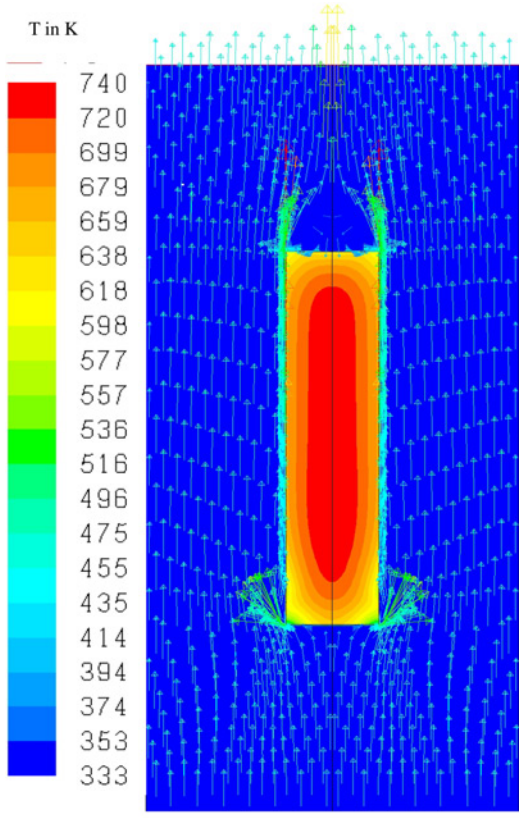

Notes: $V_{ax} = 0.3\,ms^{-1}$, $T_{liq} = 333\,K$ and $t = 7.5\,s$

Figure 13.
Temperature field in the cylinder and flow field vectors in the fluid

phases can be calculated in good agreement with experiments. The heat transfer coefficient is calculated with an error less than 30 per cent. This reasonable agreement is in the range of other boiling models describing the boiling phases separately (Celata *et al.*, 2006), but here the simulation for the different boiling phases is done within one single model. The maximum heat transfer (CHF) is underestimated, but this effect is less important in heat treatment quenching application because of its short duration (less than 1 s). More important is the correct representation where and when the CHF point is located on the specimen surface because it indicates the transition from film boiling to nucleated boiling.

4. Summary/conclusions

Flow boiling heat transfer during quenching is modelled based on CFDs. The mixture model as a two-phase model in combination with a Bubble Crowding Model is implemented. Additional model implementations have been incorporated that describe the vapour formation at the superheated solid-liquid interface and the recondensation process of vapour at the subcooled vapour-liquid interface. Also the mass transfer rate in the different boiling phases and the microconvection effect in the nucleate boiling phase resulting from bubble growth and detachment are incorporated.

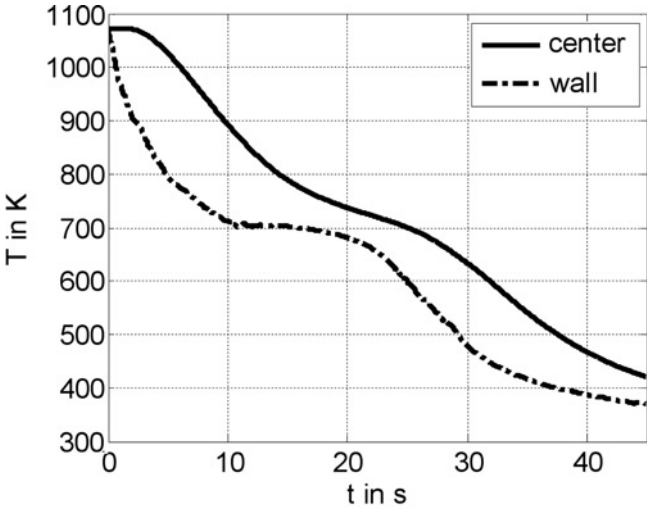

Notes: $V_{ax} = 0.3\,ms^{-1}$ and $T_{liq} = 293\,K$

Figure 14.
Local cylinder temperature at the half height, transient simulation

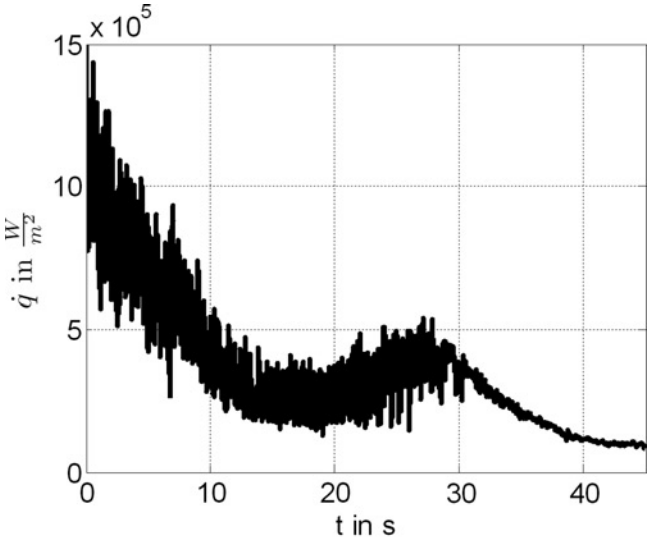

Notes: $V_{ax} = 0.3\,ms^{-1}$ and $T_{liq} = 293\,K$

Figure 15.
Heat flux, transient simulation

In the simulations, vapour is generated in hot fluid zones instead of single nucleation sites at the wall. Therefore, the governing conservation equations for mass, momentum and energy are extended by sink and source terms in the continuity and energy equations and by a momentum source at the wall.

The developed model provides an approach for calculating the complete heat transfer distribution during different boiling regimes in quenching applications. Reasonable computational efforts are needed, though local models may predict the

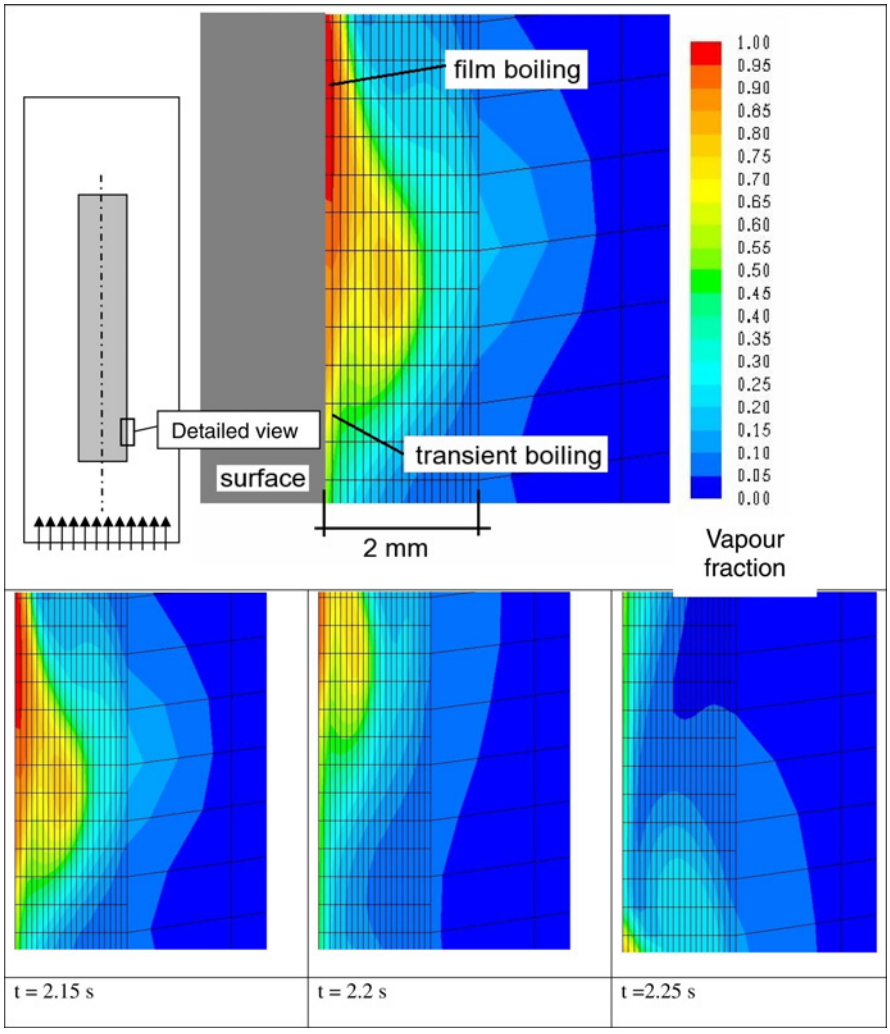

Figure 16.
Collapsing of the vapour film

details of the physical processes more correctly (nucleation sites, super heat for onset nucleate boiling, evaporation in the microzone).

The derived flow boiling model allows transient simulations of all boiling conditions and heat transfer regimes during the quenching process as:

- stable film boiling;
- transient boiling;
- nucleate boiling; and
- pure convection.

The model provides first results for the process design to avoid uneven cooling caused by film boiling.

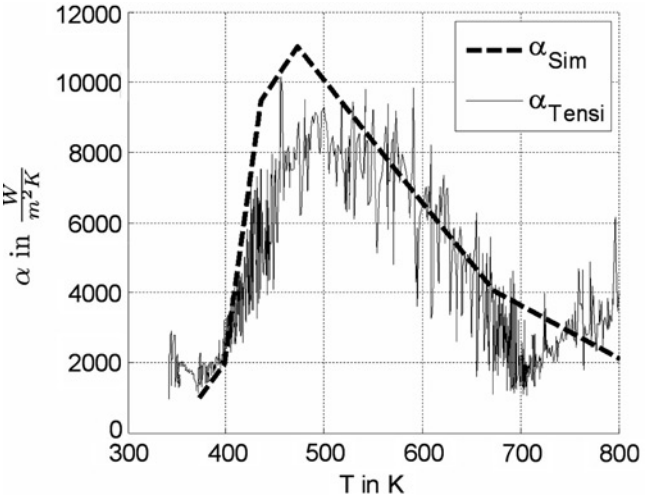

Figure 17.
Heat transfer coefficient in comparison with experimental results from Stich and Tensi (1995)

The steady-state behaviour for the heat transfer rate has been simulated and compared to literature data. Transient simulation runs have been performed for the quenching of a circular cylinder that indicate the usefulness of the derived model for the analysis and technical implementation of the simulation tool in engineering applications for quenching processes.

References

Auracher, H. and Marquardt, W. (2002), "Experimental studies of boiling mechanisms in all boiling regimes under steady-state and transient conditions", *International Journal of Thermal Sciences*, Vol. 41 No. 7, pp. 586-98.

Auracher, H. and Marquardt, W. (2004), "Heat transfer characteristics and mechanisms along entire boiling curves under steady-state and transient conditions", *International Journal of Heat and Fluid Flow*, Vol. 25 No. 2, pp. 223-42.

Celata, G.P., Cumo, M. and Mariani, A. (1997), "Geometrical effects on the subcooled flow boiling critical heat flux", *Revue Générale de Thermique*, Vol. 36 No. 1, pp. 807-14.

Celata, G.P., Cumo, M. and Mariani, A. (2007), "Spray cooling heat flux in quenching of hot surface", *Proceedings to International Conference Multiphase Flow 2007*, *Leipzig*, pp. S4_Wed_D_44.

Celata, G.P. *et al.* (2006), "Boiling heat transfer and boiling equipment", *Proceedings of the International Advanced Summer Course*, *Darmstadt*, *28 August-1 September*.

Cooper, M.G. (1984), "Saturation nucleate pool boiling – a simple correlation", *Institution of Chemical Engineers (IchemE) Symposium Series*, Vol. 86, pp. 786-93, Institute of Mechanical Engineers, London.

Dhir, V.K. (2001), "Numerical simulations of pool-boiling heat transfer", *AICHE Journal*, Vol. 47 No. 4, pp. 813-34.

Dhir, V.K. and Gihun, S. (2007), "Some unexplored aspects of pool and flow boiling", *Proceedings of the International Conference Multiphase Flow*, *Leipzig*, p. PL4.

Elias, E. and Yadigaroglu, G. (1977), "A general one-dimensional model for conduction-controlled rewetting of a surface", *Nuclear Engineering and Design*, Vol. 42 No. 2, pp. 185-94.

Esmaeeli, A. and Tryggvason, G. (2004), "Computations of film boiling. Part I: numerical method", *International Journal of Heat and Mass Transfer*, Vol. 47 No. 25, pp. 5451-61.

Fluent (2006), *Fluent 6.3 User's Guide*, Fluent, Lebanon, NH.

Rohsenow, W.M. (1952), "A method of correlating heat transfer data for surface boiling of liquids", *Journal of Heat Transfer, Transactions on ASME*, Vol. 74 No. 8, pp. 969-76.

Schmidt, R. and Fritsching, U. (2007), "Multi-scale modelling and experimental validation of gas quenching processes", *European Conference on Heat Treatment*, *Berlin*, *25-27 April*.

Stephan, P. and Fuchs, T. (2007), "Local heat flow and temperature fluctuations in wall and fluid in nucleate boiling systems", *Heat and Mass Transfer*, available at: www.springerlink.com/content/rqw8485472000j1t/fulltext.html, DOI: 10.1007/s00231-007-0320-1 (accessed 14 August).

Stich, A. and Tensi, H.M. (1995), "Wärmeübetragung und Temperaturverteilung mit Benetzungsablauf beim Tauchkühlen", *HTM Härterei-Technische Mitteilungen*, Vol. 50 No. 1, p. S. 31.

VDI, Verein Deutscher Ingenieure (2002), *VDI-Wärmeatlas*, 9th ed., Springer, Berlin.

Weisman, J. and Pei, B.S. (1983), "Prediction of critical heat flux in flow boiling at low qualities", *International Journal of Heat and Mass Transfer*, Vol. 26 No. 10, pp. 1463-77.

Yadigaroglu, G. (2005), "Computational fluid dynamics for nuclear applications: from CFD to multi-scale CMFD", *Nuclear Engineering and Design*, Vol. 235, pp. 2-4.

Corresponding author
Fabian Krause can be contacted at: krause@iwt.uni-bremen.de